AD

TECHNICAL REPORT ARCCB-TR-99013

THERMAL DAMAGE AND SHEAR FAILURE OF CHROMIUM PLATED COATING ON AN A723 STEEL CANNON TUBE

JOHN H. UNDERWOOD
ANTHONY P. PARKER

JULY 1999

US ARMY ARMAMENT RESEARCH,
DEVELOPMENT AND ENGINEERING CENTER
CLOSE COMBAT ARMAMENTS CENTER
BENÉT LABORATORIES
WATERVLIET, N.Y. 12189-4050

APPROVED FOR PUBLIC RELEASE; DISTRIBUTION UNLIMITED

DISCLAIMER

The findings in this report are not to be construed as an official Department of the Army position unless so designated by other authorized documents.

The use of trade name(s) and/or manufacturer(s) does not constitute an official endorsement or approval.

DESTRUCTION NOTICE

For classified documents, follow the procedures in DoD 5200.22-M, Industrial Security Manual, Section II-19, or DoD 5200.1-R, Information Security Program Regulation, Chapter IX.

For unclassified, limited documents, destroy by any method that will prevent disclosure of contents or reconstruction of the document.

For unclassified, unlimited documents, destroy when the report is no longer needed. Do not return it to the originator.

REPORT DOCUMENTATION PAGE

Form Approved
OMB No. 0704-0188

1. AGENCY USE ONLY *(Leave blank)*	2. REPORT DATE	3. REPORT TYPE AND DATES COVERED
	July 1999	Final

4. TITLE AND SUBTITLE

THERMAL DAMAGE AND SHEAR FAILURE OF CHROMIUM PLATED COATING ON AN A723 STEEL CANNON TUBE

5. FUNDING NUMBERS

PRON No. F18X2011M21A

6. AUTHOR(S)

John H. Underwood and Anthony P. Parker (Royal Military College of Science, Cranfield University, Swindon, UK)

7. PERFORMING ORGANIZATION NAME(S) AND ADDRESS(ES)

U.S. Army ARDEC
Benet Laboratories, AMSTA-AR-CCB-O
Watervliet, NY 12189-4050

8. PERFORMING ORGANIZATION REPORT NUMBER

ARCCB-TR-99013

9. SPONSORING / MONITORING AGENCY NAME(S) AND ADDRESS(ES)

U.S. Army ARDEC
Close Combat Armaments Center
Picatinny Arsenal, NJ 07806-5000

10. SPONSORING / MONITORING AGENCY REPORT NUMBER

11. SUPPLEMENTARY NOTES

To be presented at the ASME Pressure Vessels and Piping Conference, Boston, MA, 1-5 August 1999.
To be published in proceedings of the conference.

12a. DISTRIBUTION / AVAILABILITY STATEMENT

Approved for public release; distribution unlimited.

12b. DISTRIBUTION CODE

13. ABSTRACT *(Maximum 200 words)*

Degradation of the electroplated chromium coating at the bore of A723 steel cannon barrels is characterized here following cannon firing and used to model the coating failure process. Transient thermal stresses due to firing are calculated using one-dimensional heat flow analysis and used as input to a shear failure model of the coating/substrate couple. The cracking array that develops in the coating and substrate with repeated thermal cycles, the configuration of cracked segments of the coating, and the elevated temperature properties of the coating and substrate are considered in the shear failure model. Accordingly, the coating failure behavior predicted from the model is compared with the observations of coating failure mechanisms from actual fired cannon tubes. The results of the investigation show that growth of hydrogen cracks in the steel under the chromium coating allows broadening of cracks in the coating, and subsequent shear failure of the steel under a segment of coating due to transient thermal stresses. Loss of coating segments then leads to rapid hot gas erosion of the steel and loss of function of the cannon tube. The objective is to model the final critical phase of thermal damage imparted to a chromium coating on a cannon bore that leads to the separation of a segment of coating.

14. SUBJECT TERMS

Thermal Damage, Chromium Plating, Alloy Steel, Cannon Tube, Hydrogen Cracks, Thermal Stress, Residual Stress

15. NUMBER OF PAGES

18

16. PRICE CODE

17. SECURITY CLASSIFICATION OF REPORT	18. SECURITY CLASSIFICATION OF THIS PAGE	19. SECURITY CLASSIFICATION OF ABSTRACT	20. LIMITATION OF ABSTRACT
UNCLASSIFIED	UNCLASSIFIED	UNCLASSIFIED	UL

TABLE OF CONTENTS

Page

ACKNOWLEDGEMENTS iii

INTRODUCTION 1

DAMAGE CHARACTERIZATION 1

ANALYSIS 4

Comparison of Failure Mechanisms 4
Shear Failure 6
Bending Failure 6
Crack Growth Failure 7
Critical *(l/t)* for Failure 7
Applied Thermal Shear Stress 7

RESULTS 9

Temperature and Normal Stress Distributions 9
Shear Stresses; Crack Opening and Rate Effects 11

CLOSING 13

Summary of Observed Damage 13
Summary of Analysis 13

REFERENCES 15

TABLES

1. Summary of Cannon Firing Conditions and Damage to Chromium Coating; at 1.5-m Forward of Breech End of Cannon 3

LIST OF ILLUSTRATIONS

1. Polished and etched section from near-bore region of cannon A at 1.5-m forward of breech end of tube; longitudinal orientation (100X) 2

2. Polished and etched section from near-bore region of cannon B (130X) 2

3. Sketch of idealized segment of chromium coating and some nomenclature 4

4. Failure mechanisms for chromium coating subjected to thermal load 5

5. Temperature distribution in chromium coating of cannon A at 1.5-m forward of breech, for various times after round passage 9

6. Biaxial compressive thermal stresses in chromium coating of cannon A at 1.5-m forward of breech, for various times 10

7. Biaxial compressive thermal stresses in chromium coating of cannon A at 1.5-m forward of breech, for various times; 0.5 percent strain required for crack closure 10

8. Segment shear stress for cannons A and B adjacent to cracks with and without gap 11

9. Effect of temperature rise time due to round passage on chromium temperature at various times and depths for cannon A 12

10. Effect of temperature rise time due to round passage on segment shear stress for cannons A and B 12

ACKNOWLEDGEMENTS

The authors are pleased to acknowledge the metallographic work of C. Rickard and the help in evaluating observations and analysis by S. Sopok, E. Troiano, and G.N. Vigilante of the U.S. Army Armament RD&E Center.

INTRODUCTION

Thermal damage of the electroplated chromium coating on a cannon bore has been a problem for decades. Ahmad (ref 1) has reviewed many aspects of gun barrel erosion, including the important role of chromium coatings in controlling thermal damage due to firing. In the past decade the thermal damage problem has become critical due to a significant increase in the combustion temperatures of cannon firing. Sopok et al. (ref 2) have reported the high combustion gas temperatures used in modern tank cannons and the thermochemical erosion modeling methods now used to describe the degradation of cannon bore surfaces.

Recently, thermomechanical analysis and fracture mechanics analysis of cannon firing damage has been undertaken to characterize and model the thermal damage and cracking that occurs in the chromium coating and underlying steel at and just below the cannon bore surface. Underwood et al. (ref 3) have showed metallographic results of hydrogen cracks undermining the chromium coating and described the thermomechanics that predicts yielding, phase transformation, creation of residual stress, and growth of hydrogen cracks in the steel just below the chromium/steel interface. Underwood, Vigilante, and Troiano (ref 4) have calculated temperature and residual stress distributions for two high levels of combustion gas temperature and showed that observed phase transformation and hydrogen crack depths agree with calculations from the models.

The objective here is to model the final critical phase of thermal damage imparted to a chromium coating on a cannon bore—the separation of a segment of coating from the underlying steel. Once a segment separates, hot gas erosion quickly destroys the utility of the cannon, so separation is the critical event. In prior work, the temperature and applied and residual stress distributions have been described and used to predict crack growth in the steel with crack surfaces normal to the bore surface. Metallographic results summarized here show coating segments typically separate with the failure surface parallel to the bore surface and just below the coating/steel interface. The transient thermal stresses from one-dimensional heat flow are used here to model the observed failure process near the interface, using various cracking and shear failure modes and elevated temperature properties and failure strengths of chromium and steel. It will be seen that the failure mode near the interface that occurs at lowest applied thermal stress is failure by shear. Thus, it is emphasized.

DAMAGE CHARACTERIZATION

Figures 1 and 2 summarize some key features of the thermal damage that occurs in the near-bore region of a modern tank cannon. Each of the photomicrographs shows a typically 0.15-mm thick electroplated chromium layer near the top of the photo, and the 1100 MPa yield strength A723 steel below. Figure 1 shows thermal effects in both coating and steel of cannon A, notably a subtle 1322°K chromium recrystallization to a depth about two-thirds through the coating, and a quite clear 1022°K steel transformation to a depth about 0.07-mm below the interface. The use of these effects as accurate local temperature measurements to verify the thermomechanical modeling has been described in References 3 and 4. Another feature clearly shown in Figure 1, and one that will have importance later, is the wide variation in crack widths

in the chromium coating. Note that the cracks that extend deep into the steel have great width, whereas the cracks that extend only through or part through the transformed layer of steel have much less width. This and other features were carefully measured in dozens of photomicrographs such as that of Figure 1.

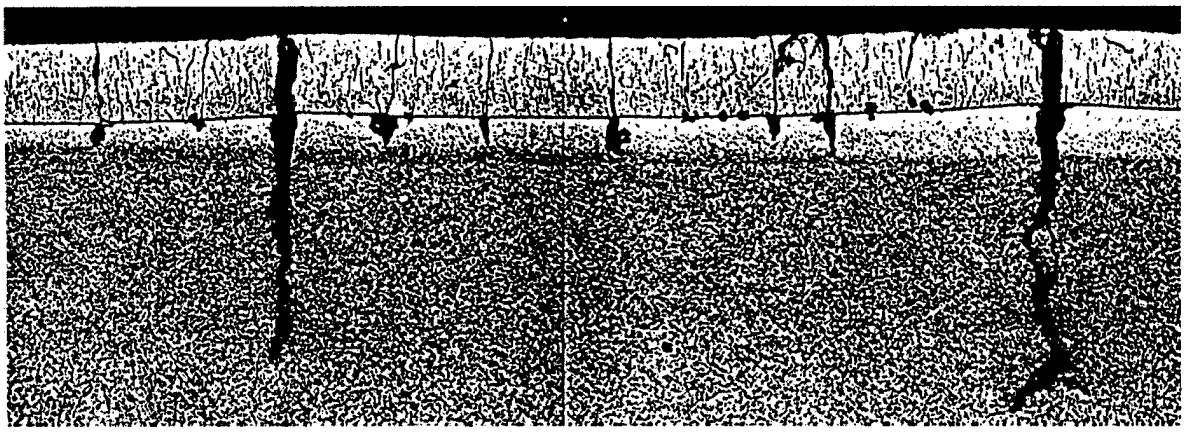

Figure 1. Polished and etched section from near-bore region of cannon A at 1.5-m forward of breech end of tube; longitudinal orientation (100X).

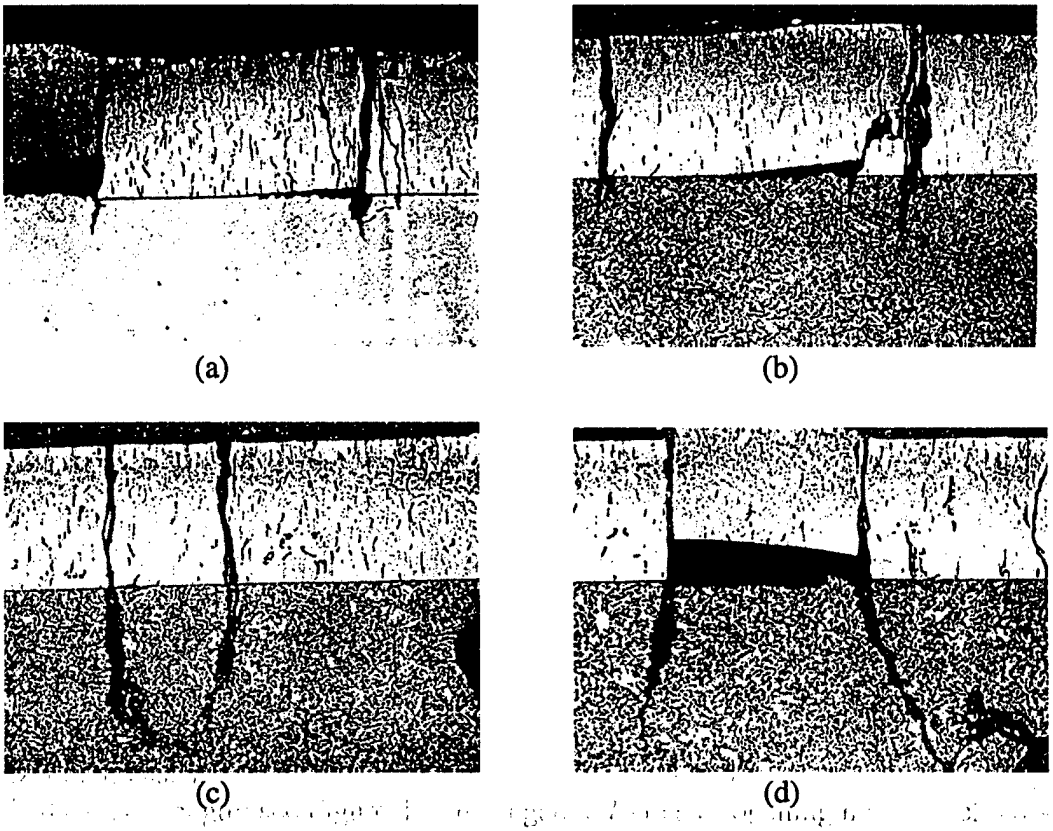

Figure 2. Polished and etched section from near-bore region of cannon B (130X). Figures 2(a) and (b) are longitudinal orientation at 1.5-m forward of breech end of tube. Figures 2(c) and (d) are transverse orientation at 0.7-m forward of breech end of tube.

Mean values of the measurements are summarized in Table 1, which also gives information on the two cannon firing conditions considered here. The combustion gas temperatures and the configuration of the coating and cracks within it will be used in thermal stress failure modeling of a segment of coating, in sections that follow. Note that, although the coating thickness varies somewhat, the relative average spacing and width of cracks within the coating are relatively constant. Also, it must be stated that the values of crack width, w, relative to crack spacing, l, $w/l = 0.04 - 0.05$ in Table 1, are approximate. The apparent crack widths measured from photomicrographs could be affected by rounding during metallographic polishing, even though care has been taken to avoid this and other problems. The important points are that there is considerable opening of some cracks and relatively little in others. The effects of significant stress redistribution around open cracks and thermal stress buildup around closed cracks will be considered in the upcoming analysis.

Table 1. Summary of Cannon Firing Conditions and Damage to Chromium Coating; at 1.5-m Forward of Breech End of Cannon

	Gas Temperature (T_G)	Coating Thickness (t)	Crack Spacing (l/t)	Crack Width (w/l)
Cannon A	3820°K	0.12-mm	1.53	0.05
Cannon B	3000°K	0.17-mm	1.46	0.04

Examples of progressive damage in cannon B are shown in Figure 2. The samples shown were etched to reveal the chromium recrystallization, and all but sample (a) were also etched to reveal the steel microstructure. As expected, considering the lower gas temperature of cannon B, the extent of chromium recrystallization (shown as a light etching region) was much less than that for cannon A. And also, as expected, there was more recrystallization closer to the hotter breech end of the cannon, (c) and (d), than farther from the breech, (a) and (b). Finally, there is no indication in Figure 2 of steel transformation, which again, is consistent with the lower gas temperature of cannon B.

Damage processes that lead to the critical separation of a chromium segment are shown in Figure 2, and are interpreted as follows: Figures 2(a) and (b) each show a segment about half separated, accompanied by concentrated cracking damage, and uplifting of the chromium at the separated end of the segment. Each of these features suggests that a substantial contact has occurred between the separated end of the segment and the neighboring segment. The upcoming analysis will explore thermal stresses that could account for both the segment contact and separation. Figure 2(c) shows an example of a potential segment separation caused by undermining of a segment of chromium by two cracks that join. Figure 2(d) shows a segment that has separated and in the process of final departure. Note in each of the cases of partial or complete separation—(a), (b), and (d)—an open region is present adjacent to the segment to facilitate separation. In (a) there is an already separated segment (to the left), and in (b) and (d) there are widely open cracks. The presence of an open region adjacent to a separating segment is generally noted and appears to be required to facilitate separation.

One other feature of the firing damage in cannon B should be noted. There was considerably more loss of chromium segments at 1.5-m forward of the breech end, compared to the loss at 0.7-m forward of the breech end. This was clearly seen in macrophotos of the bore surface, not shown here. This was puzzling, because, due to the basic effect of expansion of gases, gas temperatures are expected to decrease with distance from the breech end of a cannon, and the expected decrease was verified by the chromium recrystallization results in Figure 2. The effect of rate of application of thermal stresses as determined by round velocity will be considered in the upcoming analysis, in an effort to solve this puzzle.

Figure 3 shows an idealized representation of a segment of chromium coating along with some of its key configurational features and their nomenclature. A representation is depicted of the transient compressive thermal stress that occurs when the chromium is heated by firing and is restrained from thermal expansion. An open crack is often observed adjacent to a segment, shown at right in the sketch, which requires that there are no thermal stresses on this face of the segment. The stresses and likelihood of separation along the bottom of the segment, A-B, is the focus of the upcoming analysis.

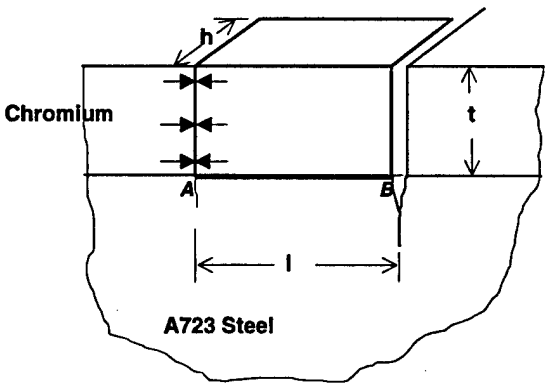

Figure 3. Sketch of idealized segment of chromium coating and some nomenclature.

ANALYSIS

Comparison of Failure Mechanisms

Separation of a segment of chromium coating as pictured in Figures 2(a) and (b) can be envisioned to occur by either a progressive crack growth process along the bottom of the segment or by a shear or bending overload failure along the base of the segment. A partial separation like that in Figures 2(a) or (b) would be explained as an interrupted crack growth or overload failure. Considering that the duration of firing stresses, both mechanical and thermal, is a small fraction of a second, an interrupted failure seems quite possible.

Figure 4 summarizes key features of three failure mechanisms considered for a segment of chromium coating. Mechanisms 1 or 2, shear or bending failure of the segment, would occur if the shear or bending stress near the base of the segment exceeded the critical material strength in this area. Cannon experience has shown (ref 1) that adhesive strength of properly electroplated chromium exceeds the tensile strength of chromium, which in turn exceeds the tensile strength of cannon steel. Thus, it is believed that the tensile strength of the A723 steel would control failure of the segment for mechanisms 1 and 2. Mechanism 3, crack growth failure, would occur if either the opening or shear mode stress intensity factor exceeded the corresponding fracture toughness. Analysis of small fragments of separated segments of coating with scanning electron fractography could provide supporting evidence of the various mechanisms, but this quite difficult task was beyond the scope of this work.

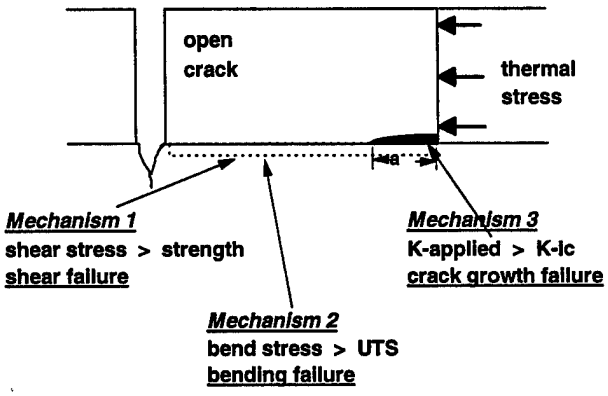

Figure 4. Failure mechanisms for chromium coating subjected to thermal load.

The presence or absence of open cracks significantly affects each of these three failure mechanisms. With no open cracks present, a shear or bending failure of a given segment would require failure of all adjoining segments, effectively greatly increasing the failure area, and thus making failure quite unlikely. Also, for the case of no open cracks, symmetry requires that shear stresses are zero on all planes parallel to the chromium/steel interface. Crack growth failure with no open cracks is also expected to be unlikely, based on the following analysis by Tada, Paris, and Irwin (ref 5) that gives opening and shear mode stress intensity factor expressions, K_I and K_{II}, for a crack configuration similar to mechanism 3, as follows:

$$K_I = -0.561\ \sigma_T(\pi a)^{1/2} \qquad (1)$$

$$K_{II} = +0.367\ \sigma_T(\pi a)^{1/2} \qquad (2)$$

where σ_T in our case is the mean compressive thermal stress applied to the end of the segment and 'a' is the crack length; see Figure 4. The negative K_I makes opening mode crack growth impossible, and the relatively low value of K_{II} makes shear mode crack growth unlikely, when there are no open cracks. Based on the above rationale and our metallographic observations of

open cracks, the remaining analysis discussed here is for cases where open cracks are present in firing-damaged chromium coatings.

Shear Failure

A shear failure along the base of a coating segment with an open crack can be described by an expression for the average shear stress, τ, on the base area of the segment, as follows:

$$\tau = \sigma_{U\text{-}C}(th)/(lh) \tag{3}$$

where $\sigma_{U\text{-}C}$ is the ultimate tensile strength of the chromium, the term (th) is the area of the segment end that is subjected to thermal stress, and (lh) is the shear area of the segment base; see again Figures 3 and 4. Equation (3) includes the assumption that the thermal stress on the segment end is at the level of the ultimate tensile stress of the chromium; later results will address this assumption. Using a criterion for shear failure of the steel adjacent to the segment base

$$\tau_{MAX} = \sigma_{U\text{-}S}/2 \tag{4}$$

where $\sigma_{U\text{-}S}$ is the ultimate tensile strength of the steel. Combining equation (3) with equation (4) gives an expression for the critical segment length-to-thickness ratio, $(l/t)_{SH}$, for shear failure of a segment as follows:

$$(l/t)_{SH} = 2\sigma_{U\text{-}C}/\sigma_{U\text{-}S} \tag{5}$$

Note that the l/t ratio for shear failure depends only on the ratio of ultimate tensile strengths of the two materials.

Bending Failure

A bending failure can be envisioned in which crack growth occurs along the base of a coating segment as observed in Figure 2, as opposed to crack growth normal to the coating plane typical of other types of bending. An expression for this type of bending stress, σ, at the base area of the segment is

$$\sigma = 6(\sigma_{U\text{-}C}\, t^2 h/2)/hl^2 \tag{6}$$

where $(\sigma_{U\text{-}C}\, t^2 h/2)$ is the bending moment. Equation (6) is combined with the failure criterion for bending failure, $\sigma = \sigma_{U\text{-}S}$, to obtain an expression for the critical segment length-to-thickness ratio, $(l/t)_{BD}$, for bending failure of a segment

$$(l/t)_{BD} = (3\sigma_{U\text{-}C}/\sigma_{U\text{-}S})^{1/2} \tag{7}$$

Again, the l/t ratio for bending failure depends only on the ratio of ultimate tensile strengths of the two materials.

Crack Growth Failure

Equation (1) showed that opening mode crack growth was not possible for the case of closed cracks. However, for open cracks and with a bending stress, as discussed in the previous section, crack growth can occur. Tada , Paris, and Irwin (ref 5) give an expression for opening mode stress intensity factor, K_I, for a homogeneous uncracked ligament of size l, subjected to bending moment, M, as

$$K_I = 4M/hl^{3/2} \tag{8}$$

Equation (8) is not directly applicable to the case here, because chromium and steel have different properties. However, considering that the elastic modulus of chromium is within about 20 percent that of A723 steel, equation (8) is believed to provide a reasonable measure of K. Using the expression for M from equation (6) and the criterion for crack growth, K_I = fracture toughness, K_{Ic}, gives an expression for the critical segment length-to-thickness ratio, $(l/t)_{CK}$, for crack growth failure of a segment

$$(l/t)_{CK} = (2\sigma_{U\text{-}C}\, t^{1/2}/K_{Ic})^{2/3} \tag{9}$$

Critical (l/t) for Failure

Evaluation of the critical ratios of (l/t) for failure can be accomplished using equations (5), (7), and (9) and using the following material property and coating configuration values: $\sigma_{U\text{-}C}$ = 2000 MPa; $\sigma_{U\text{-}S}$ = 1000 MPa; $K_{Ic\text{-}S}$ = 50 MPa $m^{1/2}$; t = 0.12 mm. These material properties were selected to be lower than room temperature values, to account, albeit in an approximate way, for the effects of elevated temperature. The t value is the chromium plate thickness of cannon A. The calculated critical (l/t) ratios for failure are:

$$(l/t)_{SH} = 4.0; \qquad (l/t)_{BD} = 2.5; \qquad (l/t)_{CK} = 0.9$$

The most important implication of these (l/t) results is that shear failure of a chromium plate segment is clearly the most likely mechanism, because failure can occur with a significantly larger segment in shear, compared to bending or crack growth. So for any given length of segment relative to thickness, shear failure will be the first to occur. Thus, shear failure will be the emphasis of subsequent analysis and the results that follow.

Applied Thermal Shear Stress

The transient temperature distribution in the near-bore region of a fired cannon can be well described using one-dimensional heat flow analysis available in texts on heat transfer, such as Incropera and DeWitt (ref 6). This type of analysis was used in prior work (ref 4) to obtain a closed-form expression for the transient temperature distribution, $T\{x, \phi\}$ for any point, x, below the bore surface and any time, ϕ. The expression repeated here for reference is

$$[T\{x,\phi\} - T_i]/[T_{gas} - T_i] = erfc[x/2(\beta\phi)^{1/2}] - [exp[hx/k + h^2\beta\phi/k^2]]$$

$$\times[erfc[x/2(\beta\phi)^{1/2} + h(\beta\phi)^{1/2}/k]] \quad (10)$$

where

$T\{x,\phi\}$ is the transient temperature distribution for any point, x, below the surface and any time, ϕ.
T_i is the initial temperature of the solid.
T_{gas} is the temperature of the gas (varying with location).
erfc is the complementary Gaussian error function.
β is thermal diffusivity (m^2/s).
h is thermal convection coefficient (W/m^2K).
k is thermal conductivity (W/mK).

The prior work gave an expression for the biaxial transient normal thermal stress, σ_T, in the plane parallel to the bore surface for any temperature $T\{x,\phi\}$. The expression, with one modification, is

$$\sigma_T = E\alpha[T\{x,\phi\} - T_i - T_C]/[1 - \nu] \quad (11)$$

where E is elastic modulus (GPa), α is thermal expansion coefficient ($1/K$), ν is Poisson's ratio, and T_C is a modification to account for the closure of an open crack. If, for example, a thermal elastic strain of 0.5 percent were required to close a crack, the effective closure temperature, T_C, could be easily calculated from equation (11) and then used in subsequent calculations of σ_T to account for the effect of the initially open and later closed cracks on thermal stresses.

The normal thermal stresses, as described by equation (11), can be used to calculate the applied shear stress, τ_{APP}, on the base of the segment of chromium coating, as follows:

$$\tau_{APP} = (\sum\sigma_T\{x_I - x_{i-1}\}/2)(t/l) \quad (12)$$

The summation $\sum\sigma_T\{x_I - x_{i-1}\}/2$ over an arbitrary 'i' slices through the depth of the coating and gives the average normal stress applied to the segment. The (t/l) term accounts for the ratio of normal area to shear area; see equation (3). In the results to follow, a 0.12-mm coating thickness, as observed with cannon A, was divided into twelve 0.01-mm thick slices, to provide an accurate calculation of the thermal shear stress applied to the base of a coating segment. The effects of two potentially important variables on the shear stress at the base of the segment are considered in the results. These are crack opening, already discussed in relation to damage characterization, and the varying rate of application of thermal stresses due to the increasing velocity of the round as it moves down the cannon.

RESULTS

Temperature and Normal Stress Distributions

Temperature distributions for various times, following initial application of hot gases to the bore surface of the chromium coating, are shown in Figure 5, for a location 1.5-m forward of the breech end of cannon A. For these and all other results shown, the following thermal properties and other parameters were used in equations (10) and (11), as appropriate:

T_i is the initial temperature of the cannon, 300°K.
β is thermal diffusivity, 1.35 $E-05$ m^2/s.
k is thermal conductivity, 65.4 W/mK.
E is elastic modulus, 200 GPa.
α is thermal expansion coefficient, 9.4 E - 06/K.
ν is Poisson's ratio, 0.3.

These values were obtained (or estimated in some cases) from References 6 and 7 for chromium at 1000°K, as a representative temperature at the base of a chromium segment undergoing failure. Previous work (ref 3) noted that significant variations in material properties produced relatively minor shifts in derived temperature distributions. Based on this, the model results discussed here are believed to give a good representation of the critical failure at the base of the chromium segments. The thermal convection coefficient, h, used for all results was 400,000 W/m^2K, which was selected to produce the known 1022°K steel transformation temperature at the same depth in the analysis as that observed from metallography (ref 4).

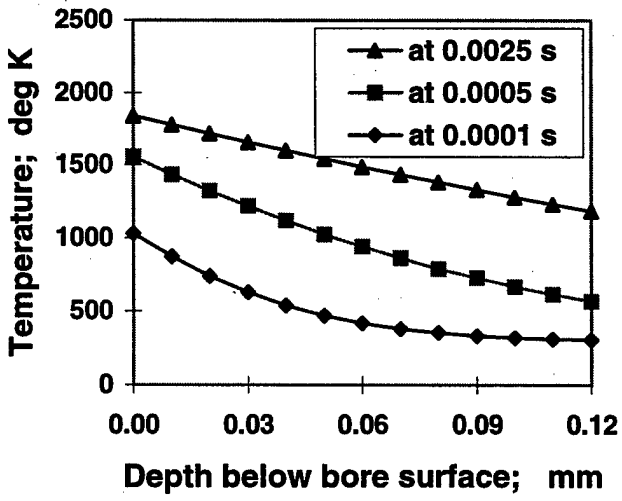

Figure 5. Temperature distribution in chromium coating of cannon A at 1.5-m forward of breech, for various times after round passage.

The temperature distributions from Figure 5 were used to calculate normal thermal stress distributions using equation (11), with no effect of any crack closure at the contact end of the chromium segment, that is, with $T_C = 0$. See Figure 6. Note that except for the shortest times after the heating begins with the passage of the round, the biaxial thermal stresses near the surface are above the estimated 2000 MPa compressive strength of the chromium. Thus, plastic deformation of the chromium is indicated, and this is consistent with the uplifting of the chromium and the assumption of stresses equal to the tensile strength of the chromium, both noted earlier. It is clear that there is sufficient thermal stress to do considerable damage to the chromium coating.

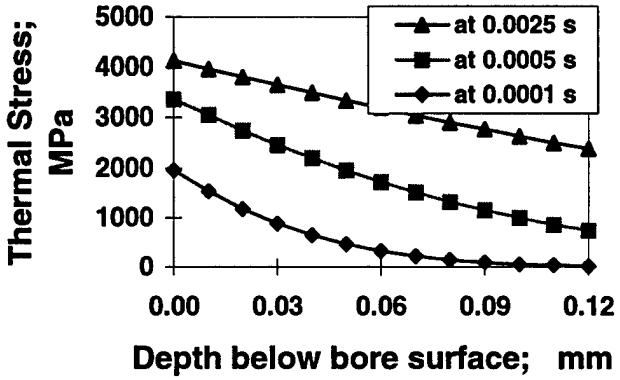

Figure 6. Biaxial compressive thermal stresses in chromium coating of cannon A at 1.5-m forward of breech, for various times.

Figure 7 considers the effect of a partially open crack at the contact end of the segment on the thermal compressive stress. The calculations summarized by equation (11) and Figure 6 were repeated with $T_C = 672°K$, the value associated with 0.5 percent thermal expansion. The reduced thermal compressive stresses shown in Figure 7, compared to those in Figure 6, would be expected for a crack that required a 0.5 percent expansion to close.

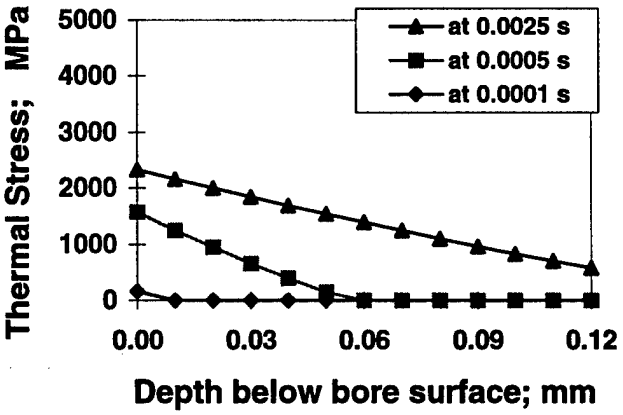

Figure 7. Biaxial compressive thermal stresses in chromium coating of cannon A at 1.5-m forward of breech, for various times; 0.5 percent strain required for crack closure.

Shear Stresses; Crack Opening and Rate Effects

Equation (12) can be used to calculate the applied thermal shear stress, τ_{APP}, near the interface of the segment of chromium coating, with and without a partially open crack as discussed above. Results for cannons A and B, with and without the 0.5 percent gap at the contact side of the segment, are shown in Figure 8. As with the normal stresses, there is a significant decrease in the applied shear stresses due to the gap. These results indicate that shear failure of a chromium segment is more likely for segments separated initially by a tightly *closed crack.* Recalling the earlier discussion, a widely *open crack* adjacent to a segment is associated with failure, so the complete requirement for segment shear failure may be a closed or nearly closed crack on one side of the segment and a widely open crack on the other side. A review of Figure 1 shows examples of segments with this arrangement.

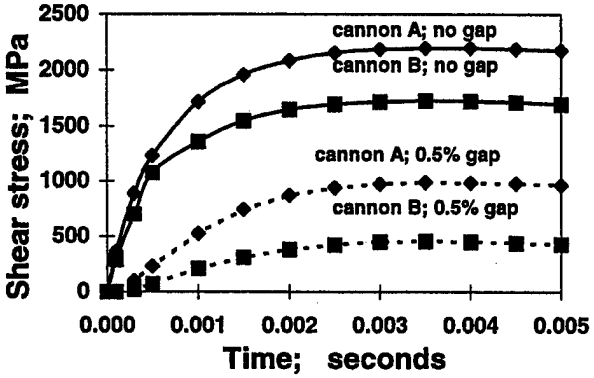

Figure 8. Segment shear stress for cannons A and B adjacent to cracks with and without gap.

The last question for discussion here related to thermal shear failure of chromium segments is the effect of the time rate of thermal stress application on failure. The round velocity and the resulting rate of application of hot gases to the bore surface of the chromium vary by several multiples of ten during the first meter of travel. This variation in velocity leads to variation in the temperature rise time of the gases at the bore surface. For example, if the distance over which the temperature rises from T_i to T_{gas} is 0.001-m and the round velocity is 200 m/s, then the temperature rise time would be 0.05 ms. This rise time and one ten times longer, corresponding to a lower-round velocity, are considered in the following analysis of segment shear stress. Figure 9 shows effects of the two different temperature rise times on the temperature distributions calculated from equation (10), and Figure 10 shows the resulting segment shear stresses using equations (11) (with $T_C = 0$) and (12). Both temperature and shear stress are considerably reduced, but only within the time period corresponding to the rise time. Note that dT/dt and $d\tau_{APP}/dt$ are much lower for the slower rise time. This lesser amount of thermal shock associated with the lower round velocity could account for the observed lesser amount of chromium loss at 0.7-m forward of the breech compared with 1.5-m forward, discussed earlier. The high values of segment shear stress that occur later in time are not affected by temperature rise time, and thus cannot account for the observed differences in chromium loss.

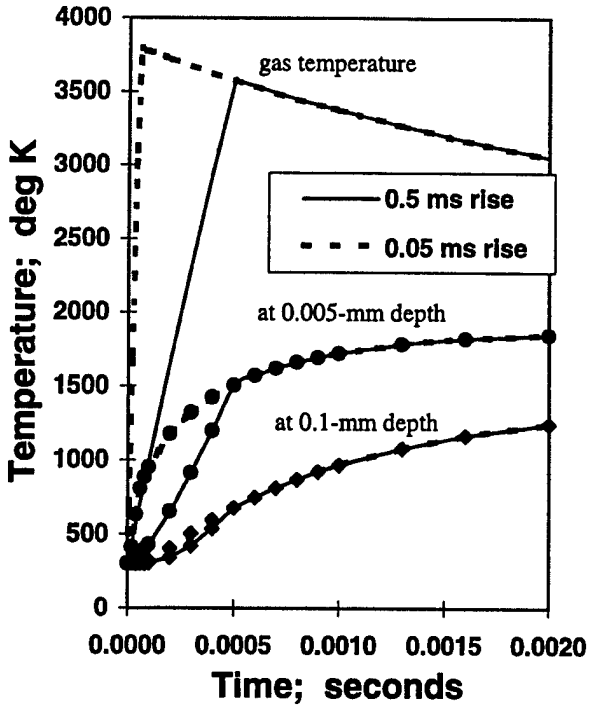

Figure 9. Effect of temperature rise time due to round passage on chromium temperature at various times and depths for cannon A.

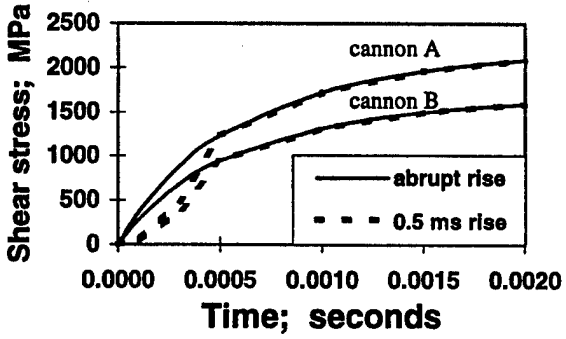

Figure 10. Effect of temperature rise time due to round passage on segment shear stress for cannons A and B.

CLOSING

Summary of Observed Damage

Observations suggest that severe firing damage of the chromium coating and adjacent steel at a cannon bore occurs by the following mechanisms:

1. Biaxial thermal compressive stresses in both materials and compressive yielding and phase transformation in one or both materials

2. Cracking and segmentation of the chromium by thermomechanical damage, and growth and opening of cracks by hydrogen-assisted cracking of the steel

3. Thermal shear failure of the steel just below the base of a chromium segment that is adjacent to an open hydrogen crack

4. Separation of a chromium segment followed by rapid hot gas erosion of the exposed steel and loss of function of the cannon

Summary of Analysis

Thermomechanical analysis was focused on the chromium segment failure portion of the severe firing damage that has been observed in cannons. The analysis is summarized as follows:

1. Three mechanisms of chromium segment separation were compared: bending failure, crack growth failure, and shear failure of the steel at the base of a segment that is adjacent to an open crack. Shear failure was predicted to occur for significantly larger coating segments than for bending or crack growth, making shear the most likely coating segment failure mechanism.

2. One-dimensional heat flow analysis using representative elevated temperature properties was used to calculate temperatures and associated biaxial normal stresses in the chromium. Temperatures of nearly 2000°K were calculated and verified using known transformation temperatures for chromium and steel. Compressive stress in excess of 4000 MPa was consistent with observations of severe contact damage and yielding in the chromium.

3. Applied shear stresses in the steel at the base of a chromium segment were calculated by summing the normal stresses in several layers. Shear stresses as high as twice the expected shear strength of the steel were calculated, giving support to the observations of shear-like failure of chromium segments.

4. A model of a partially open crack that requires 0.5 percent thermal expansion for closure predicted 55 to 77 percent reductions in the applied shear stress at the base of a chromium segment.

5. A model of reduced-temperature rise time caused by slow cannon round velocity showed a significant decrease in applied thermal shear stress loading rate, $d\tau_{APP}/dt$, and no effect on the maximum value of applied shear stress for a chromium segment, τ_{APP}.

REFERENCES

1. Ahmad, I., "The Problem of Gun Barrel Erosion; An Overview," in *Gun Propulsion Technology*, (Ludwig Stiefel, Ed.), Vol. 109 of *Progress in Astronautics and Aeronautics*, AIAA, Washington, 1988, pp. 311-355.

2. Sopok, S., O'Hara, P., Vottis, P., Pflegl, G., Rickard, C., and Loomis, R., "Erosion Modeling of the 120-mm M256/M829A2 Gun System," *Proceedings of 1997 ADPA Gun and Ammunition Symposium*, San Diego, CA, 7-10 April 1997.

3. Underwood, J.H., Parker, A.P., Cote, P J., and Sopok, S., "Compressive Thermal Yielding Leading to Hydrogen Cracking in a Fired Cannon, *Journal of Pressure Vessel Technology,* Vol. 121, 1999, pp. 116-120.

4. Underwood, J.H., Vigilante, G.N., and Troiano, E., "Thermomechanical Model of Hydrogen Cracking at Heat-Affected Cannon Bore Surfaces," *Proceedings of International Workshop on Hydrogen Management for Welding Applications*, Ottawa, Canada, 6-8 October 1998.

5. Tada, H., Paris, P.C., and Irwin, G.R., *The Stress Analysis of Cracks Handbook*, Paris Productions, Inc., St. Louis, MO, 1985, pp. 8.10, 9.1.

6. Incropera, F.P., and. DeWitt, D.P., *Introduction to Heat Transfer,* Wiley, New York, 1985, pp. 202-205; 669-670.

7. Smithells, C.J., *Metals Reference Book*, Butterworths, Washington, 1962.

TECHNICAL REPORT INTERNAL DISTRIBUTION LIST

	NO. OF COPIES
TECHNICAL LIBRARY ATTN: AMSTA-AR-CCB-O	5
TECHNICAL PUBLICATIONS & EDITING SECTION ATTN: AMSTA-AR-CCB-O	3
OPERATIONS DIRECTORATE ATTN: SIOWV-ODP-P	1
DIRECTOR, PROCUREMENT & CONTRACTING DIRECTORATE ATTN: SIOWV-PP	1
DIRECTOR, PRODUCT ASSURANCE & TEST DIRECTORATE ATTN: SIOWV-QA	1

NOTE: PLEASE NOTIFY DIRECTOR, BENÉT LABORATORIES, ATTN: AMSTA-AR-CCB-O OF ADDRESS CHANGES.

TECHNICAL REPORT EXTERNAL DISTRIBUTION LIST

	NO. OF COPIES
DEFENSE TECHNICAL INFO CENTER ATTN: DTIC-OCA (ACQUISITIONS) 8725 JOHN J. KINGMAN ROAD STE 0944 FT. BELVOIR, VA 22060-6218	2
COMMANDER U.S. ARMY ARDEC ATTN: AMSTA-AR-WEE, BLDG. 3022 AMSTA-AR-AET-O, BLDG. 183 AMSTA-AR-FSA, BLDG. 61 AMSTA-AR-FSX AMSTA-AR-FSA-M, BLDG. 61 SO AMSTA-AR-WEL-TL, BLDG. 59 PICATINNY ARSENAL, NJ 07806-5000	 1 1 1 1 1 2
DIRECTOR U.S. ARMY RESEARCH LABORATORY ATTN: AMSRL-DD-T, BLDG. 305 ABERDEEN PROVING GROUND, MD 21005-5066	 1
DIRECTOR U.S. ARMY RESEARCH LABORATORY ATTN: AMSRL-WM-MB (DR. B. BURNS) ABERDEEN PROVING GROUND, MD 21005-5066	 1
COMMANDER U.S. ARMY RESEARCH OFFICE ATTN: TECHNICAL LIBRARIAN P.O. BOX 12211 4300 S. MIAMI BOULEVARD RESEARCH TRIANGLE PARK, NC 27709-2211	 1

	NO. OF COPIES
COMMANDER ROCK ISLAND ARSENAL ATTN: SIORI-SEM-L ROCK ISLAND, IL 61299-5001	 1
COMMANDER U.S. ARMY TANK-AUTMV R&D COMMAND ATTN: AMSTA-DDL (TECH LIBRARY) WARREN, MI 48397-5000	 1
COMMANDER U.S. MILITARY ACADEMY ATTN: DEPT OF CIVIL & MECH ENGR WEST POINT, NY 10966-1792	 1
U.S. ARMY AVIATION AND MISSILE COM REDSTONE SCIENTIFIC INFO CENTER ATTN: AMSAM-RD-OB-R (DOCUMENTS) REDSTONE ARSENAL, AL 35898-5000	 2
COMMANDER U.S. ARMY FOREIGN SCI & TECH CENTER ATTN: DRXST-SD 220 7TH STREET, N.E. CHARLOTTESVILLE, VA 22901	 1

NOTE: PLEASE NOTIFY COMMANDER, ARMAMENT RESEARCH, DEVELOPMENT, AND ENGINEERING CENTER, BENÉT LABORATORIES, CCAC, U.S. ARMY TANK-AUTOMOTIVE AND ARMAMENTS COMMAND, AMSTA-AR-CCB-O, WATERVLIET, NY 12189-4050 OF ADDRESS CHANGES.